Changes in action potentials and intracellular ionic homeostasis in a ventricular cell model related to a persistent sodium current in SCN5A mutations underlying LQT3

Georges Christé, Mohamed Chahine, Philippe Chevalier, Michal Pásek

For: Progress in Biophysics and Molecular Biology; focused issue

Changes in action potentials and intracellular ionic homeostasis in a ventricular cell model related to a persistent sodium current in SCN5A mutations underlying LQT3.

G Christé[1], M Chahine[2], P Chevalier[3], M Pásek [4,5]

[1]INSERM, ADR Lyon, Lyon F-69003 France

[2] Le Centre de Recherche Université Laval Robert-Giffard and Department of Medicine, Laval University, Québec, Canada

[3]Unité de Cardiologie et Soins Intensifs, Hôpital Cardiovasculaire et Pneumologique L. Pradel, Lyon, F-69003 France; INSERM, ERITM107, Lyon, F-69003 France

[4]Institute of Thermomechanics, Czech Academy of Sciences, Brno, Czech Republic

[5]Department of Physiology, Faculty of Medicine, Masaryk University, Brno, Czech Republic

Address for correspondence

Georges Christé,
Present address:
Université Claude Bernard – Lyon 1,
Bât. R. Dubois, 2° étage,
F-69622 Villeurbanne Cedex, France.
Tel: (33)4 78 40 00 57 Fax: (33)4 72 44 79 37
E-mail address: christe@lyon.inserm.fr

Abstract

In LQT3 patients, SCN5A mutations induce ultraslow inactivation of a small fraction of the hNav1.5 current i.e. persistent Na^+ current (I_{pNa}). We explored the time course of effects of such a change on the intracellular ionic homeostasis in a model of guinea-pig cardiac ventricular cell (Pasek et al., 2007b, this issue). Sudden addition of I_{pNa} prevented action potential (AP) repolarization when its conductance (g_{pNa}) exceeded 0.12% of the maximal conductance of fast I_{Na} (g_{Na}). With g_{pNa} at 0.1% g_{Na}, the AP duration at 90% repolarization (APD_{90}) was initially lengthened to 2.6 fold that in control. Under regular stimulation at 1 Hz it shortened progressively to 1.37 fold control APD_{90}, and intracellular $[Na^+]_i$ increased by 6% with a time constant of 106 sec. Further increasing g_{pNa} to 0.2% g_{Na} caused an immediate increase in APD_{90} to 5.7 fold that in control, which decreased to 2.2 fold that in control in 30 sec stimulation at 1 Hz. At this time diastolic $[Na^+]_i$ and $[Ca^{2+}]_i$ were respectively 34% and 52% higher than in control and spontaneous erratic SR Ca release occurred.

In the presence of I_{pNa} causing 46% lengthening of APD_{90}, the model cell displayed arrhythmogenic behaviour when external $[K^+]$ was lowered to 5 mM from an initial value at 5.4 mM. By contrast, when K^+ currents I_{Kr} and I_{Ks} were lowered in the model cell to produce the same lengthening of APD_{90}, no proarrhythmic behaviour was observed, even when external $[K^+]$ was lowered to 2.5 mM.

Keywords: Sudden death – mutation – SCN5A – long QT syndrome – model

Introduction

Mechanisms by which mutation-induced alterations of the hNav1.5 current predispose LQT3 patients to arrhythmias have been explored from an electrical point of view (Bennett et al., 1995; Clancy et al., 1999; Clancy et al., 2003; Tian et al., 2004; Henry et al., 2004; Berecki et al., 2006). However, only few works have addressed possible changes in ionic homeostasis related to increased persistent or late Na^+ current (Priori et al., 1996; Bito et al., 2006; Noble and Noble, 2006). In particular, the presence of a persistent Na^+ current (I_{pNa}) during the action potential might cause elevation of intracellular [Na^+], a condition that predisposes to calcium overload and arrhythmogenesis (Levi et al., 1997; Noble and Noble, 2006; see also Maltsev and Undrovinas, 2007 in this volume). We explored whether this effect would be quantitatively important in a computer model of cardiac ventricular myocyte. We also compared the immediate and delayed effects of introducing a persistent Na^+ current. Finally, we compared the alterations of ionic homeostasis in two modifications of the model producing equivalent AP prolongation as in symptomatic LQT (addition of a persistent Na^+ current or decreased K^+ currents) and their response to manoeuvres likely to aggravate sodium overload: tachycardia and hypokalemia. We discussed the relevance of the effects produced by the model to clinical situations. Part of this work was reported in abstract form (Christé et al., 2005; Christé et al., 2006).

Methods

A ventricular cell model that includes ionic currents, intracellular ionic homeostasis and a single compartment tubular system (Pasek et al., 2003) was modified to closely match the properties of guinea-pig ventricular cells at 37°C as described in Pasek et al., (2007b), a companion paper in this issue. This model was written and integrated under the MATLAB environment (The MathWorks). A persistent Na^+ current (termed I_{pNa} in the rest of the text) was formulated according to the description of Sakmann et al., (2000), see equations A7 to A10 in Appendix 1 to the paper by Pasek et al., (2007b) in this issue. The conductance of this current in control conditions was 0.0053 mS/cm^2.

In the first series of modelling attempts (figures 1, 2 and 3), the model was implemented with a transient outward (I_{to}) current (as in Pasek et al. 2003) to approach the ion current conditions of a human myocyte. The immediate and long term effects of introducing a persistent I_{pNa} were explored in these conditions.

In the second series of model challenges (figs 4 and 5), three versions of our model (Pasek et al., 2007b , this issue) were used. The unmodified version of the model is named the *Cont* model. In the first modification (named $+I_{pNa}$ model) of the model *Cont*, the maximal conductance of I_{pNa} (g_{pNa}) was set to 0.02 mS/cm^2 to simulate of a LQT3 condition. In a second modification (named $-I_K$ model) of model *Cont*, the maximal conductance for both I_{Kr} and I_{Ks} was reduced by 67%, to simulate a LQT1/LQT2 condition. Both modified models and the control model were run for at least 600 s cell life time to ensure that all variables had reached steady-state. For examination of the susceptibility of each modified model to generate arrhythmias in lowered extracellular $[K^+]_e$ or increased frequency, each model was run for 300 s at 1 Hz and at 3 Hz, and in each modified $[K^+]_e$ condition at 1 Hz.

Results

The control AP shown in figure 1 was recorded after 630 s cell lifetime of stimulation at 1 Hz. We then tested the addition of different amounts of I_{pNa} current. When the conductance of I_{pNa} was increased by 0.3 mS/cm^2 (which represents 1% of the maximal fast I_{Na} conductance that is 30 mS/cm^2, and is within the range of fractions of late I_{Na} produced by most 'gain of function' mutations of SCN5A), the first AP failed to repolarize (not shown, but see Undrovinas et al., 1999). The total conductance of I_{pNa} had to be less than 0.035 mS/cm^2 (0.12% of maximal fast I_{Na} conductance) for the model cell AP to repolarize. As depicted in figure 1A, after increasing I_{pNa} conductance to 0.03 mS/cm^2, the first AP at 1 Hz showed a lengthened AP duration at 90 % repolarisation (APD_{90}) that was 2.6 times that in control. Remarkably, however, as regular stimulation at 1 Hz proceeded, APD_{90} shortened to a steady-state value 1.37 times that in control, and this change was complete in 150 s. From this state, further increase of I_{pNa} conductance to 0.06 mS/cm^2 did not compromise AP repolarization (Fig 1B). The next AP in this new condition displayed a APD_{90} 5.7 times that in control. There also appeared small voltage oscillations late during the AP plateau (see below). Subsequently, and as formerly, APD_{90} decreased down to 2.2 fold that in control in 30 sec stimulation at 1 Hz. There appeared small voltage oscillations at regular intervals (delayed after depolarisations (see below).

Thus the model cell tends to compensate for a large part but not all of the lengthening of AP duration caused by the increased sustained sodium inward current. After increasing g_{pNa} to 0.03 mS/cm^2, the repolarizing currents that most prominently increased and account for shorter duration of AP at steady state in figure 1A are I_{NaK} (the electrogenic sodium-potassium pump current), I_{NaCa} (the electrogenic sodium-calcium exchanger current) and I_{KsNa} (the sodium activated potassium current). Remarkably, the I_{Ks} current that was prominent during the plateau of the first AP is greatly decreased during the AP at steady state under 1Hz stimulation (not shown). After further increasing g_{pNa} to 0.06 mS/cm^2, the extra outward currents that increased after progressive APD shortening were I_{NaCa} and I_{KsNa}, whereas the Na-K pump current did not increase further (not shown).

We next considered the most remarkable changes in ionic currents and intracellular Na^+ and Ca^{2+} handling upon suddenly increasing g_{pNa} to 0.06 mS/cm^2 (figure 2A), as such a sudden increase in I_{pNa} might occur in case of drugs altering I_{Na} inactivation (e.g.: anthopleura toxin Priori et al., 1996;

amiodarone Bito et al., 2006), but also under respiratory acidosis (Plant et al., 2006) or acute hypoxia (Ju et al., 1996; Fearon et al., 2004). As shown in figure 2A, small early after-depolarisations (EADs) are present during the plateau of the AP (arrows). These are not accompanied with reactivation of the Ca current (second panel from top in fig 2A), but are caused by spontaneous Ca release from the SR as indicated by sudden changes in $[Ca^{2+}]$ in the dyadic subspace ($[Ca^{2+}]_{isub}$), which caused $[Ca^{2+}]_i$ transients. The variations in the Na-Ca exchanger current (I_{NaCa}) during the plateau of the AP are closely related to changes in $[Ca^{2+}]_i$.

After regular stimulation at 1 Hz for 30 s, the AP had significantly shortened (figure 2 B). At this time there developed an overload of the intracellular compartment with Na^+ and of the SR with Ca^{2+} (see figure 3). Under this condition, delayed after-depolarisations (DADs) were present, concomitant with sharp increases in $[Ca^{2+}]_{isub}$ and intracellular Ca^{2+} transients. Inward changes in the Na-Ca exchanger current closely followed the changes in $[Ca^{2+}]_i$.

To further understand the build up of Na^+ overload, we compared action potentials (V_m, figure 3A) and I_{pNa} (figure 3B) in control and after stabilization at 1 Hz with addition of 0.03 and 0.06 mS/cm^2 g_{pNa}. It is readily visible that the amount of Na^+ ions entering during an AP (i.e. the area under the I_{pNa} trace) is greatly enhanced due the extra Na^+ ions carried by the added I_{pNa}, but also due to AP prolongation. The time integral of the I_{pNa} current was 8.26 that in control after addition of 0.03 mS/cm^2 g_{pNa}, 39% of which was carried during the additional AP duration versus control. After further increasing g_{pNa} to 0.06 mS/cm^2, the integral was further increased 3.2 fold (reaching 26.5 times that in control) and 73% of this was carried during additional AP duration versus control.

Intracellular $[Na^+]$ and $[Ca^{2+}]$ at end of diastole are shown respectively in panels C and D of figure 3. The progressive overload of the intracellular space with Na^+ ($[Na^+]_i$ in figure 3C) was modest after increasing g_{pNa} to 0.03 mS/cm^2 (gain of less than 1 mM from 15.4 mM to 16.3 mM) whereas after further increasing g_{pNa} to 0.06 mS/cm^2, $[Na^+]_i$ raised by 4.4 mM to reach 20.67 mM at steady-state. In both cases, the relaxation of intracellular Na^+ was slow (time constant of 106 s and 75 s respectively for the first and second increases in $[Na^+]_i$ in figure 3C, indicating that the overload builds up from beat to beat. As shown in figure 3 D, each of these progressive increases in $[Na^+]_i$ was accompanied by a parallel rise in end diastolic $[Ca^{2+}]_i$ from171 nM to 200 nM during the first period. By 30 s during the second period, at the time when the AP in figure 3A (g_{pNa} = 0.06, dotted line) was recorded, $[Ca^{2+}]_i$ was 260 nM. Shortly thereafter, $[Ca^{2+}]_i$ started to display large sudden increases (fig 4 D) that occurred again later, eventually reaching values persistently beyond 1 µM, which would

have been deleterious to a real cardiac cell. Thus the model cardiac cell could stabilize to a new steady-state with moderate sodium overload when the increase in I_{pNa} was moderate, whereas a larger I_{pNa} would cause the cell to enter a deleterious Na^+ and Ca^{2+} overload.

We so far have explored three situations: i) an instantaneous increase in I_{pNa}, that is likely to be directly arrhythmogenic, due to a large increase in AP duration leading to EADs, ii) a situation with moderate Na^+ and Ca^{2+} overload, in which AP lengthening has largely recessed and that may represent a stable adapted state, iii) a third condition when I_{pNa} was further increased might relate to a deleterious situation in which the cell may suffer from large Ca^{2+} overload.

In the next series of simulations, we explored situation ii), that might correspond to a stable symptomatic LQT3 condition that does not show arrhythmogenic behaviour *per se* but in which AP prolongation and Na^+ and Ca^{2+} overload would predispose to lethal arrhythmias triggered by other proarrhythmic events (e.g.: bradycardia, QT prolonging drugs, Wu et al., 2006). Two features might favour the output of proarrhythmic events: the prolonged AP duration was reported to be proarhythmogenic in LQT3 patients, especially at low cardiac frequencies and this has been documented in animal and computer models of LQT3 (Bennett et al., 1995; Clancy et al., 1999; Clancy et al., 2003; Tian et al., 2004; Henry et al., 2004; Berecki et al., 2006). The second factor: intracellular Na^+ overload, has received less attention. Two manoeuvres likely to further increase Na^+ overload are an increase in cardiac frequency (Pieske et al., 2002) and any action likely to block the Na-K pump, e.g. hypokalaemia, that is a known risk factor of sudden cardiac death as it increases AP duration and the incidence of EADs but also aggravates Na^+ overload.

We thus investigated the response of two modifications of our model causing similar AP prolongation, the first one due to an increase of I_{pNa}, the second to the partial block of K^+ currents I_{Ks} and I_{Kr}.

As described in the methods, a first variant (model $+I_{pNa}$) was created, that included a I_{pNa} set at 0.02 mS/cm^2 (i.e. 0.07 % of peak fast g_{Na}) to produce a APD_{90} prolongation by 46%, comparable to that seen in symptomatic patients with LQT3 syndrome (Modell et al., 2006). The properties of this model are compared with another model (model $-I_K$), with decreased repolarizing currents I_{Kr} and I_{Ks}, that achieved a similar AP prolongation at 1 Hz. The steady state APs in these two modified models are superimposed with the AP from the control model. Fig. 4, left column shows the time-course of changes in several variables during one cycle at 1 Hz stimulation frequency once the model reached dynamic stability (after 300 s cell lifetime at 1 Hz).

The APD_{90} was similar in both modified models (i.e. 223 ms for model $+I_{pNa}$ and 222 ms for model $-I_K$). This represented a 46 % prolongation of APD_{90} versus 153 ms in the *Cont* model (fig. 4a). This compares well with QTc lengthening in LQT3 subjects (Modell et al., 2006).

Fig.4b shows the magnitudes of the sum of I_{Kr} and I_{Ks} (in *Cont* and $-I_K$ models) and of I_{pNa} in $+I_{pNa}$ model. Intracellular Na^+ concentration ($[Na^+]_i$, 10.95 mM in *Cont* model - fig. 4c) increased to 12.1 mM (+10.5 %) in the $+I_{pNa}$ model whereas it decreased to 9.95 mM (-9.1 %) in the $-I_K$ model. In the $+I_{pNa}$ model, the intracellular Ca^{2+} transient ($[Ca^{2+}]_i$, fig. 4d) was larger than in *Cont* model (peak value 1.08 µM versus 0.77 µM in *Cont* model i.e. +40 %) as well as the end-diastolic intracellular Ca^{2+} value (0.11 µM versus 0.09 µM in *Cont* model i.e. +30 %). In the $-I_K$ model, these values were slightly lowered to respectively 0.73 µM (-5 %) and 0.08 µM (-8%). Correspondingly, the Ca^{2+} concentration in the uptake compartment of the SR ($[Ca^{2+}]_{SRup}$, fig. 4e) in $+I_{pNa}$ model was higher than in *Cont* model by 58 % at peak and 43 % at the end of diastole whereas in the $-I_K$ model, these values were, respectively, 10 % and 7 % lower than in *Cont* model.

Thus at a stimulation rate of 1 Hz, the presence of a persistent Na^+ current caused increase $[Na^+]_i$ and $[Ca^{2+}]_i$, whereas the model with decreased K^+ currents, although producing similar lengthening of AP duration, caused a slight decrease of these concentrations. Next, we tested the response of these models to a high stimulation rate (3 Hz, fig. 4 right column). The respective decrease in APD_{90} was 36 ms in the *Cont* model, 72 ms in the $+I_{pNa}$ model and 44 ms in the $-I_K$ model. The AP remained prolonged versus control in both modified models (fig. 4f), but this was less for the $+I_{pNa}$ model (+30 %) than for the $-I_K$ model (+53 %). These changes are similar to those in guinea pig ventricular myocytes exposed to either anthopleurin A (to enhance the late Na current) or to dofetilide (to block the potassium current I_{Kr}) when the stimulation frequency was increased from 1 Hz to 2.5 Hz(Priori et al., 1996). The time course of modified currents is shown in fig. 4g. For both modified models, the deviations of $[Na^+]_i$ (fig. 4h), $[Ca^{2+}]_i$ (fig. 4i) and $[Ca^{2+}]_{SRup}$ (fig. 4j) from levels in the *Cont* model were all amplified by the higher stimulation frequency versus those at 1 Hz. The model with persistent Na^+ current thus showed a tendency to overload the cell with Na^+ and Ca^{2+} that is enhanced at higher rates of stimulation whereas the model with decreased K^+ currents showed an opposite tendency.

Hypokalaemia is a condition reported to trigger arrhythmias in LQT patients. We tested the response of each model to gradual stepwise lowering of external K^+ concentration ($[K^+]_e$) from the control value of 5.4 mM. The results are summarized in fig. 5. The $-I_K$ model could stand lowering of

$[K^+]_e$ to 2.5 mM (fig. 5a) similarly to the *Cont* model (fig. 5b). Several values of the maximal conductance for I_{pNa} were used in the $+I_{pNa}$ model and the model run for 600 s in normal $[K^+]_e$. Then, the simulations with gradually lowered $[K^+]_e$ were run again. The results show that when g_{pNa} was set to 0.01 mS/cm^2, the model could stand $[K^+]_e$ as low as 2.5 mM and keep regular beating (fig. 5c), whereas when g_{pNa} was set to 0.018 mS/cm^2, the model became arrhythmic at 4.5 mM (fig. 5d). Model $+I_{pNa}$ with g_{pNa} at 0.02 mS/ cm^2 displayed arrhythmic behaviour at 5 mM (fig. 5e).

Thus the propensity to develop arrhythmic behaviour in response to lowered extracellular $[K^+]$ was directly related to the increased persistent sodium current and to its magnitude. It is noteworthy that even a quite low g_{pNa} (0.06 % of peak g_{Na}) is enough to enable proarrhythmic behaviour with a rather mild degree of hypokalaemia: $[K^+]_e$ lower than control by less than 1 mM. In contrast, the $-I_K$ model did not show more propensity than the *Cont* model to develop after-depolarisations under lowered $[K^+]_e$.

If these results with the $+I_{pNa}$ model would hold in LQT3 subjects, even pacing the heart (e.g. at 1 Hz) to protect from bradycardia-induced arrhythmias might not prevent a proarrhythmic action of hypokalaemia.

Discussion

Compared effects of immediate versus steady-state effects of inclusion of I_{pNa}.

Immediate effects of inclusion of a persistent Na current are pertinent to several situations that may occur in clinical settings. First some drugs provoke the appearance of long lived reopenings of fast Na channels that support a persistent I_{Na} (Priori et al., 1996; Bito et al., 2006). Furthermore, intracellular acidosis combined with a underlying SCN5A pH-sensitising mutation (Plant et al., 2006), acute thyroid hormone exposure (Wang et al., 2003) and acute hypoxia (Ju et al., 1996; Fearon et al., 2004) may all trigger the appearance of a persistent I_{Na}. As analysed in figures 1 and 2, these changes may prove directly arrhythmogenic, through early after-depolarisations (EADs) appearing as a consequence of a dramatic prolongation of AP plateau. This implies that the first minutes after exposure would represent a critical window for immediate arrhythmogenic consequences and associated risk of sudden death.

Should ventricular cells resist this initial AP prolongation, AP duration may rapidly shorten as a consequence of raised intracellular [Na^+] and increased repolarizing currents (figures 1 and 3) and this might be considered as a salvaging influence of Na^+ overload combined with an intact Na-K pump activity.

This second situation may be more pertinent to mimic the presence of a persistent I_{Na} as due to the expression of mutated SCN5A genes. Indeed, the inclusion of modified Na channels into the sarcolemmal membrane through translation and protein synthesis would in this case be progressive along time, leaving way to adaptation to the new condition, with changes in intracellular homeostasis, as illustrated here, and chronically elevated intracellular Na^+ and Ca^{2+} concentrations. These changes may not directly trigger arrhythmias but create a background rendering the cell more responsive to proarrhythmogenic manoeuvres, e.g.: bradycardia, drug-induced decrease in I_{Kr} or I_{Ks} and any manoeuvres likely to further increase I_{pNa} (see above). In addition, the present modelling points out to the increased susceptibility of a model cell to conditions favouring Na^+ overload: hypokalaemia that is a known trigger of arrhythmias causing sudden death. Another condition is tachycardia, that is known to cause increased $[Na^+]_i$ and does so more in the model cell with persistent Na current (fig 4). However, consistent with a increased ability of high heart rate to shorten the QT interval in LQT3 , the APD_{90} at 3 Hz showed twice larger shortening in the model cell with increased I_{pNa}. This may represent another positive consequence of Na^+ overload.

Our model results stress the importance of the lengthening of APD in maintaining Na^+ overload (fig 3 and related analysis), as a large part of the Na^+ inflow occurs during the late part of the AP that is in excess of the duration of control AP. As a consequence, therapeutic actions aiming at shortening AP duration without reducing I_{pNa} might be efficient in reducing Na^+ overload. However, selective inhibition if I_{pNa} would altogether correct the long QT condition and the associated Na^+ overload. Among such therapeutic agents, mexiletine, an efficient blocker of late Na current has proven efficient in preventing torsades de pointes associated with LQT3. However, mexiletine can also act as a chemical chaperone and has been found able to rescue SCN5A/M1766L mutated channels from defective trafficking (Valdivia et al., 2002). An adverse effect might occur if such an action results in an increase of the late Na current. This view is supported by recent evidence of restoration by mexiletine of normal trafficking of the trafficking defective SCN5A/T353I mutant with increased late Na current (Pfahnl et al. 2007). Such pharmacological rescue likely takes part to induction of acquired LQTs with cisapride in the case of the SCN5A/L1825P mutation (Liu et al. 2005). A recent therapeutic approach with a potent preferential blocker of late I_{Na} current through SCN5A channels, Ranolazine (Zygmunt et al., 2002; Noble and Noble, 2006, Maltsev and Undrovinas, 2007 in this volume) may not have such a potential adverse effect.

Compared ionic homeostasis changes with increased I_{pNa} current or with decreased I_K currents

The magnitude of the persistent current that was introduced in the $+I_{pNa}$ model caused an AP prolongation by 46 %, which is in the range reported for the QTc lengthening in LQT3 syndrome (Modell et al., 2006). For so doing, g_{pNa} was set to a value of 0.02 mS/cm^2 which represents 0.066 % of the maximal conductance for the fast Na^+ current. The magnitude of the persistent current for exogenously expressed mutated hNav1.5 channels amounted 1 to 6 % of the peak Na^+ current (Baroudi et al., 2000; Bezzina et al., 2001; Veldkamp et al., 2003; Chang et al., 2004). Thus only a small part of fast Na^+ channels (1.1 % to 6.6 %) would need to be mutated to account for a fraction of 0.066 % persistent Na^+ current. This is consistent with the heterozygous presence of most of such mutations (Veldkamp et al., 2003), allowing a mixed population of mutated and wild-type channels to coexist in cardiac cells of subjects bearing such mutations. It also entails that the mutated channel genes need not attain a high level of expression for causing a LQT3 phenotype. A consequence is that whenever the efficiency of expression of the mutated channels would be low, the magnitude of the persistent current may well be enough to create a state of predisposition of the heart to arrhythmogenic behaviour.

Here we obtained indication that the presence of a persistent Na^+ current causes intracellular overload in Na^+ and Ca^{2+} (fig 4). In contrast, a decrease in Na^+ and Ca^{2+} load (versus control condition) was seen when a similar AP prolongation was caused by a decrease in K^+ currents I_{Kr} and I_{Ks} (fig 4). This suggests that the proarrhythmogenic background created by these two alterations in ionic currents is different, and that LQT3 with persistent Na^+ current makes the cell more sensitive to an aggravation of Na^+ and Ca^{2+} overload. This is supported by the arrhythmogenicity of $[K^+]_e$ lowering in the $+I_{pNa}$ model that was not seen in the $-I_K$ model (fig 5). However, when g_{pNa} was decreased by 50% in the $+I_{pNa}$ model, it became resistant even to a low $[K^+]_e$ of 2.5 mM, as *Cont* and $-I_K$ models (fig 5). Thus there is a threshold magnitude of I_{pNa} below which the higher sensitivity to low $[K^+]_e$ did not appear.

Limitations of the model

It may be noted that the change introduced in our model to account for a persistent Na^+ current is not an exact image of the gain of function induced in the fast hNav1.5 current by most of the mutations causing LQT3 phenotype (Bezzina et al., 2001; Veldkamp et al., 2003). In particular, voltage shifts of the steady-state inactivation versus voltage relation and changes in the kinetics and/or voltage dependence of fast inactivation of the hNav1.5 current were not taken into account here. This was purposely done to explore the effects of a persistent Na^+ current per se on ionic homeostasis. Nevertheless, the complete set of changes for a given mutation should be explored to test whether the effects outlined here are altered. Another simplification is that the equations used here for the persistent Na^+ current do not account for the ultra-slow inactivation present in the persistent current of mutated channels (Bennett et al., 1995; Baroudi et al., 2000; Chang et al., 2004). However, as the time constant of this inactivation was several fold longer than the duration of APs in the present model, the magnitude of the persistent Na^+ current should be negligibly altered within the duration of an AP.

The model that we used includes a representation of the transverse-axial tubular system (TATS) and the related distributions of ion transfer mechanisms (Pasek et al., 2007b). We used this model because, in this respect, it is a likely more accurate description of a ventricular cardiac myocyte than previous models (see review by Pasek et al., 2007a, in this issue). We have shown in a former study that the presence of the TATS would retard the proarrhythmic effect of progressive hypokalaemia (Pasek et al., 2002). However, the possible effects of the presence of the transverse axial tubular system (TATS) in our model were not explored here.

The basic frequency of the model at 1 Hz was in the upper range of heart rates reported for LQT3 subjects that show bradycardia related to the persistent I_{Na} in sinus node cells (Veldkamp et al., 2003).

The present results were obtained in a model of guinea-pig ventricular cell and may not readily hold for a human cardiac cell. In particular, the frequency-related increase in $[Na^+]_i$ reported for control human cardiomyocytes (Pieske et al., 2003), was not seen in our model when frequency was increased from 1 to 3 Hz.

In our model, a single type of cell was modelled whereas in the real ventricular wall three main types of cells are present: epicardial, endocardial and mid-myocardial cells (Antzelevitch et al., 2001). There are differences between these cell types in the expression of the persistent I_{Na} current (Sakmann et al., 2000; Zygmunt et al., 2001) of the fast I_{Na} (Li et al., 2002; Antzelevitch et al., 2006) and of other currents (Antzelevitch et al., 2001). As a result, these cells have different AP durations and should respond differently to the presence of an equal amount of persistent I_{Na} current arising from mutated Na^+ channels. Furthermore, intracellular ionic homeostasis also varies among these cell types, in particular, intracellular $[Na^+]$ at rest is different as well as the activity of the Na-K pump (Gao et al., 2005), so that the incidence of a given amount of I_{pNa} shall differ also for this reason. However, the expression of the mutated channels may also be different among cell types. In the syncitial tissue, the differences in action potential durations between ventricular cells subtypes may be damped owing to electrotonic interaction (Conrath et al., 2004; Henry et al., 2004). This may not be the case for differences in $[Na^+]_i$, owing to the small equivalent length constant of transcellular Na^+ diffusion (Gao et al., 2005). These features should obviously be taken into account in a more rigorous modelling of the effects of persistent I_{Na} on each of these cell types, and on the syncitial tissue.

Conclusions

The persistence of quite a small fraction of the peak I_{Na} current (1/1000th) is enough to sizably lengthen APs in a ventricular GP myocyte model. This is relevant to the triggering of arrhythmias by an acute increase of a persistent I_{Na} current (drug, hypoxia, acidosis), but probably not to the LQT3 condition, in which the gain of function of mutated SCN5A channels would appear progressively over at least several hours.

A persistent I_{Na} directly contributes to raise intracellular [Na^+] and thereby favours intracellular [Ca^{2+}] overload, in addition to the AP lengthening per se. When the cell can adapt to this condition, a stable state of proarrhythmogenic condition is met. This is probably a closer image of the stable state of a LQT3 condition, that predisposes the cell to arrhythmogenic behaviour with additional conditions such as hypokalaemia.

Acknowledgement

Georges Christé is grateful for the support of a research grant by the "Fédération des Maladies Orphelines" (Paris). Michal Pásek acknowledges the support from project AV0Z 20760514 from the Institute of Thermo-mechanics of the Czech Academy of Sciences. Mohamed Chahine acknowledges the support from Heart and Stroke Foundation of Québec (HSFQ) and the Canadian Institutes of Health Research, MT-13181.

References

Antzelevitch, C. and Belardinelli, L., 2006. The role of sodium channel current in modulating transmural dispersion of repolarization and arrhythmogenesis. J. Cardiovasc. Electrophysiol. 17 Suppl 1, S79-S85.

Antzelevitch, C. and Fish, J., 2001. Electrical heterogeneity within the ventricular wall. Basic Res. Cardiol. 96, 517-527.

Baroudi, G. and Chahine, M., 2000. Biophysical phenotypes of SCN5A mutations causing long QT and Brugada syndromes. FEBS Lett. 487, 224-228.

Bennett, P.B., Yazawa, K., Makita, N., George, A.L., Jr., 1995. Molecular mechanism for an inherited cardiac arrhythmia. Nature 376, 683-685.

Berecki, G., Zegers, J.G., Bhuiyan, Z.A., Verkerk, A.O., Wilders, R., van Ginneken, A.C.G., 2006. Long-QT syndrome-related sodium channel mutations probed by the dynamic action potential clamp technique. J. Physiol. (Lond) 570, 237-250.

Bezzina, C.R., Rook, M.B., Wilde, A.M., 2001. Cardiac sodium channel and inherited arrhythmia syndromes. Cardiovasc. Res. 49, 257-271.

Bito, V., Dauwe, D., Verdonck, F., Mubagwa, K., Sipido, K.R., 2006. The amiodarone derivative, 2-Methyl-3-(3,5-diiodo-4- carboxymethoxybenzyl)benzofuran (KB130015) induces a Na^+-dependent increase of $[Ca^{2+}]$ in ventricular myocytes. J. Pharmacol. Exp. Ther. 316, 162-168.

Chang, C.C., Acharfi, S., Wu, M.H., Chiang, F.T., Wang, J.K., Sung, T.C., Chahine, M., 2004. A novel SCN5A mutation manifests as a malignant form of long QT syndrome with perinatal onset of tachycardia/bradycardia. Cardiovasc. Res. 64, 268-278.

Christé, G., Chahine, M., Chevalier, P., Pasek, M., 2006. Changes in intracellular ionic homeostasis related to persistent hNav1.5 sodium current in SCN5A mutations underlying LQT3: a model study. Biophys. J. 90, 98-Plat-

Christé, G., Restier, L., Chahine, M., Chevalier, P., Pasek, M., 2005. Effects of a persistent sodium current through mutated hNav1.5 sodium channels on intracellular ionic homeostasis in a ventricular cell model. Comput. Cardiol. 32, 997-1000.

Clancy, C.E. and Rudy, Y., 1999. Linking a genetic defect to its cellular phenotype in a cardiac arrhythmia. Nature 400, 566-569.

Clancy, C.E., Tateyama, M., Liu, H., Wehrens, X.H., Kass, R.S., 2003. Non-equilibrium gating in cardiac Na^+ channels: an original mechanism of arrhythmia. Circulation 107, 2233-2237.

Conrath, C.E., Wilders, R., Coronel, R., de Bakker, J.M., Taggart, P., de Groot, J.R., Opthof, T., 2004. Intercellular coupling through gap junctions masks M cells in the human heart. Cardiovasc. Res. 62, 407-414.

Fearon, I.M. and Brown, S.T., 2004. Acute and chronic hypoxic regulation of recombinant hNav1.5 a subunits. Biochem. Biophys. Res. Commun. 324, 1289-1295.

Gao, J., Wang, W., Cohen, I.S., Mathias, R.T., 2005. Transmural gradients in Na/K pump activity and $[Na^+]_i$ in canine ventricle. Biophys. J. 89, 1700-1709.

Henry, H. and Rappel, W.J., 2004. The role of M cells and the long QT syndrome in cardiac arrhythmias: Simulation studies of reentrant excitations using a detailed electrophysiological model. Chaos 14, 172-182.

Ju, Y.K., Saint, D.A., Gage, P.W., 1996. Hypoxia increases persistent sodium current in rat ventricular myocytes. J. Physiol. (Lond) 497, 337-347.

Levi, A.J., Dalton, G.R., Hancox, J.C., Mitcheson, J.S., Issberner, J., Bates, J.A., Evans, S.J., Howarth, F.C., Hobai, I.A., Jones, J.V., 1997. Role of intracellular sodium overload in the genesis of cardiac arrhythmias. J. Cardiovasc. Electrophysiol. 8, 700-721.

Li, G.R., Lau, C.P., Shrier, A., 2002. Heterogeneity of sodium current in atrial vs epicardial ventricular myocytes of adult guinea pig hearts. J. Mol. Cell. Cardiol. 34, 1185-1194.

Liu, K., Yang, T., Viswanathan, P.C., Roden, D.M., 2005. New mechanism contributing to drug-induced arrhythmia: rescue of a misprocessed LQT3 mutant. Circulation 112, 3239-3246.

Maltsev, V.A. and Undrovinas, A., 2007. Late sodium current in failing heart: friend or foe? Prog. Biophys. Mol. Biol. Present issue,

Modell, S.M. and Lehmann, M.H., 2006. The long QT syndrome family of cardiac ion channelopathies: a HuGE review. Genet. Med. 8, 143-155.

Noble, D. and Noble, P.J., 2006. Late sodium current in the pathophysiology of cardiovascular disease: consequences of sodium-calcium overload. Heart 92 Suppl 4, iv1-iv5.

Pasek, M., Christé, G., Simurda, J., 2002. Arrhythmogenic effect of extracellular K^+-depletion is prevented by the transverse-axial tubular system in a ventricular cardiac cell model. Scripta Medica 75, 179-186.

Pasek, M., Christé, G., Simurda, J., 2003. A quantitative model of cardiac ventricular cell incorporating the transverse-axial tubular system. Gen. Physiol. Biophys. 22, 355-368.

Pasek, M., Simurda, J., Christe, G., Orchard, C., 2007a. Modelling the cardiac transverse-axial tubular system. Prog. Biophys. Mol. Biol. Present issue,

Pasek, M., Simurda, J., Orchard, C.H., Christé, G., 2007b. A model of the guinea-pig ventricular cardiomyocyte incorporating a transverse-axial tubular system. Prog. Biophys. Mol. Biol. Present issue,

Pfahnl, A.E., Viswanathan, P.C., Weiss, R., Shang, L.L., Sanyal, S., Shusterman, V., Kornblit, C., London, B., Dudley, S.C., Jr., 2007. A sodium channel pore mutation causing Brugada syndrome. Heart Rhythm 4, 46-53.

Pieske, B. and Houser, S.R., 2003. $[Na^+]_i$ handling in the failing human heart. Cardiovasc. Res. 57, 874-886.

Pieske, B., Maier, L.S., Piacentino, V., III, Weisser, J., Hasenfuss, G., Houser, S., 2002. Rate dependence of $[Na^+]_i$ and contractility in nonfailing and failing human myocardium. Circulation 106, 447-453.

Plant, L.D., Bowers, P.N., Liu, Q., Morgan, T., Zhang, T., State MW, Chen, W., Kittles, R.A., Goldstein, S.A., 2006. A common cardiac sodium channel variant associated with sudden infant death in African Americans, SCN5A S1103Y. J. Clin. Invest. 116, 430-435.

Priori, S.G., Napolitano, C., Cantu, F., Brown, A.M., Schwartz, P.J., 1996. Differential response to Na^+ channel blockade, beta-adrenergic stimulation, and rapid pacing in a cellular model mimicking the SCN5A and HERG defects present in the long-QT syndrome. Circ. Res. 78, 1009-1015.

Sakmann, B.F., Spindler, A.J., Bryant, S.M., Linz, K.W., Noble, D., 2000. Distribution of a persistent sodium current across the ventricular wall in guinea pigs. Circ. Res. 87, 910-914.

Tian, X.L., Yong, S.L., Wan, X., Wu, L., Chung, M.K., Tchou, P.J., Rosenbaum, D.S., Van Wagoner, D.R., Kirsch, G.E., Wang, Q., 2004. Mechanisms by which SCN5A mutation N1325S causes cardiac arrhythmias and sudden death in vivo. Cardiovasc. Res. 61, 256-267.

Undrovinas, A.I., Maltsev, V.A., Sabbah, H.N., 1999. Repolarization abnormalities in cardiomyocytes of dogs with chronic heart failure: role of sustained inward current. Cell. Mol. Life Sci. 55, 494-505.

Valdivia, C.R., Ackerman, M.J., Tester, D.J., Wada, T., McCormack, J., Ye, B., Makielski, J.C., 2002. A novel SCN5A arrhythmia mutation, M1766L, with expression defect rescued by mexiletine. Cardiovasc. Res. 55, 279-289.

Veldkamp, M.W., Wilders, R., Baartscheer, A., Zegers, J.G., Bezzina, C.R., Wilde, A.A., 2003. Contribution of sodium channel mutations to bradycardia and sinus node dysfunction in LQT3 families. Circ. Res. 92, 976-983.

Wang, Y.G., Dedkova, E.N., Fiening, J.P., Ojamaa, K., Blatter, L.A., Lipsius, S.L., 2003. Acute exposure to thyroid hormone increases Na^+ current and intracellular Ca^{2+} in cat atrial myocytes. J. Physiol. (Lond) 546, 491-499.

Wu, L., Shryock, J.C., Song, Y., Belardinelli, L., 2006. An increase in late sodium current potentiates the proarrhythmic activities of low-risk QT-prolonging drugs in female rabbit hearts. J. Pharmacol. Exp. Ther. 316, 718-726.

Zygmunt, A.C., Eddlestone, G.T., Thomas, G.P., Nesterenko, V.V., Antzelevitch, C., 2001. Larger late sodium conductance in M cells contributes to electrical heterogeneity in canine ventricle. Am. J. Physiol. 281, H689-H697.

Legends to figures

Figure 1: Changes in APs after increasing I_{pNa}. **A**: From steady-state at 1 Hz (SS Control, continuous line), g_{pNa} was increased from 0.0053 to 0.03 mS/cm^2, the model was then run at 1 Hz. The first subsequent AP (1st AP, dotted line) and the AP at steady-state after 600 s (SS AP, dashed line) are superimposed. **B**: g_{pNa} was subsequently increased to 0.06 ms/cm^2, the first (1st AP 0.06, dotted line) and steady-state (SS AP 0.06, dashed line) APs are superimposed with the control AP (grey trace) and the steady-state AP with 0.03 mS/cm^2 g_{pNa} (SS AP 0.03).

Figure 2: From upper to lower panels in A and B: action potentials (Vm), L-type Ca current (I_{Ca}), Na-Ca exchange current (I_{NaCa}), Ca^{2+} concentrations in the dyadic subspace ($[Ca^{2+}]_{isub}$) and the intracellular space ($[Ca^{2+}]_i$). A) When the persistent current was suddenly increased from 0.03 mS/cm^2 to 0.06 mS/cm^2. B) After 30 seconds regular stimulation under this new condition. Arrows in the top panel in A denote EADs. In the second panel from top in A and B, the I_{Ca} trace was shown with its full magnitude (vertical scale on the left) and also with a 40 fold magnification (denoted x40, vertical scale on the right).

Figure 3: Progressive changes in intracellular $[Na^+]$ ($[Na^+]_i$ panel C) and intracellular $[Ca^{2+}]$ ($[Ca^{2+}]_i$ panel D) that accompany the stabilization towards the shortened APs represented in panel A. The traces of I_{pNa} corresponding to APs in A are shown in panel B.

Figure 4. Ouput data from models *Cont* (continuous lines), $+I_{pNa}$ (doted lines) and $-I_K$ (dashed lines) after 600 s of regular stimulation at 1 Hz (left column) or at 3 Hz (right column) in the I-clamp mode. Upper row: action potentials (Vm), second row show the sum of I_{Ks} and I_{Kr} currents in the *Cont* model and in the $-I_K$ model, whereas the dotted line shows the I_{Nap} current in model $+I_{Nap}$ only.

Figure 5. APs in low $[K^+]_e$ at 1 Hz stimulation frequency. **a**: in the *Cont* model after 300 s in 2.5 mM $[K^+]_e$. **b**: in the $-I_K$ model after 300 s in 2.5 mM $[K^+]_e$. **c**: in the $+I_{pNa}$ model with g_{pNa}=0.01 mS/cm^2 after 300 s in 2.5 mM $[K^+]_e$. **d**: in the $+I_{pNa}$ model with g_{pNa}=0.018 mS/cm^2 during the first 4 s of simulation in 4.5 mM $[K^+]_e$, after 300 s regular activity in 5.0 mM $[K^+]_e$ (not shown). **e**: in the $+I_{pNa}$ model with g_{pNa}=0.02 mS/cm^2 during the first 4 s of simulation at 5.0 mM $[K^+]_e$, applied from steady-state at 5.4 mM $[K^+]_e$ (not shown).

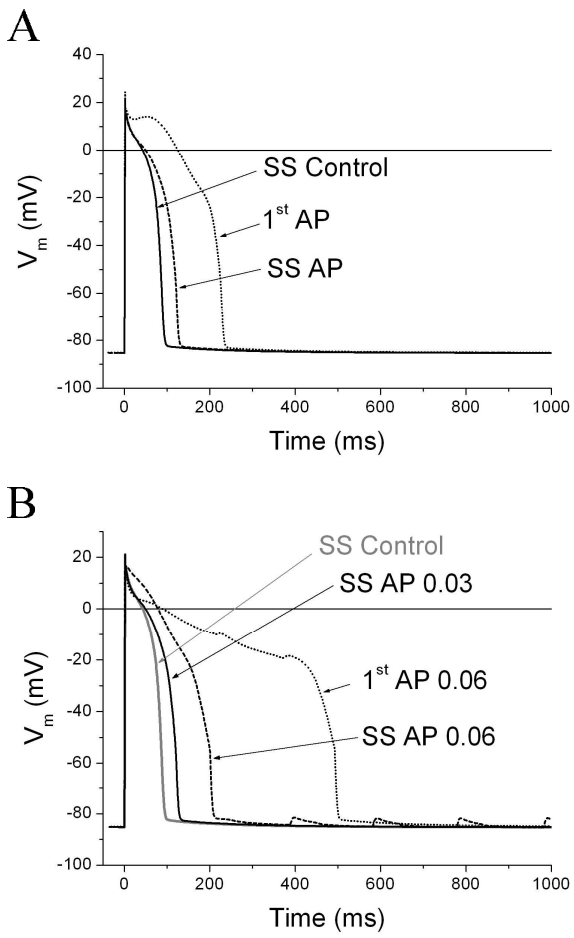

Figure 1 Christé et al. PBMB 2007

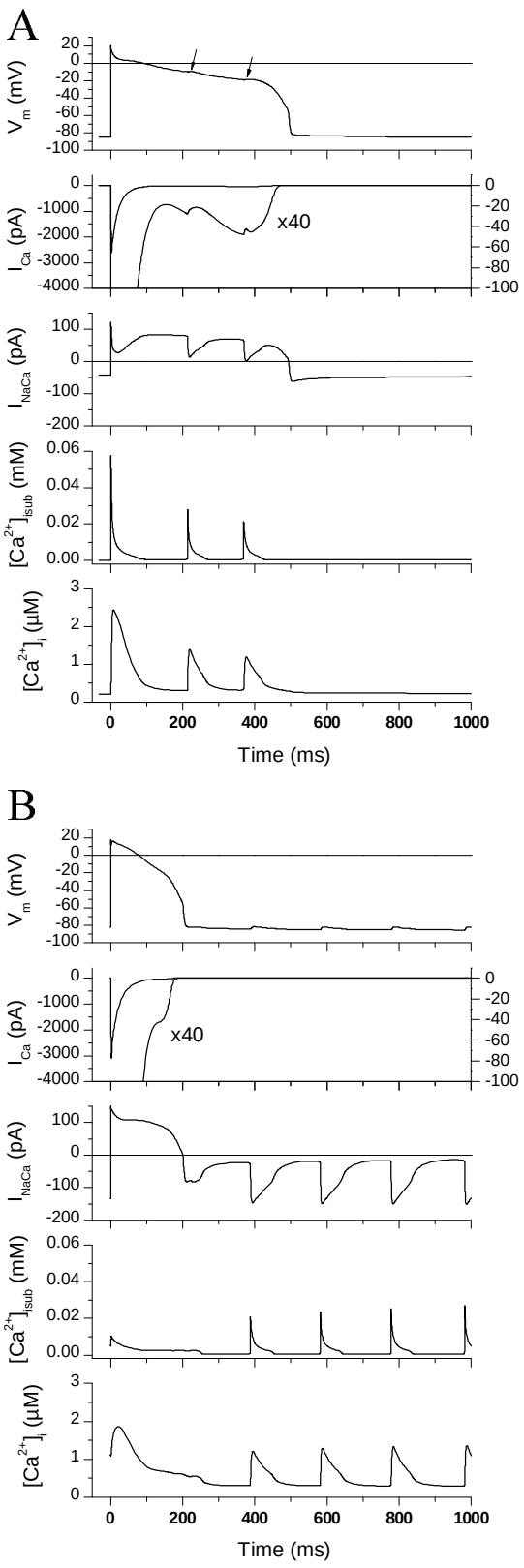

Figure 2 Christé et al. PBMB 2007

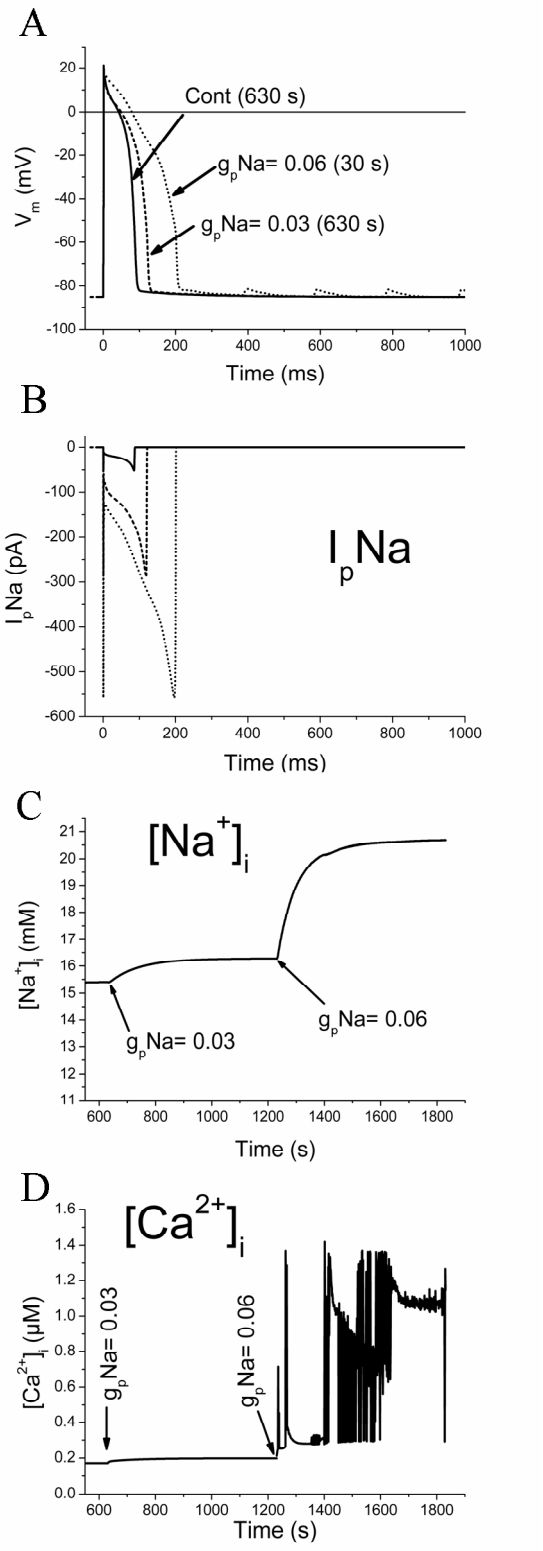

Figure 3 Christé et al. PBMB 2007

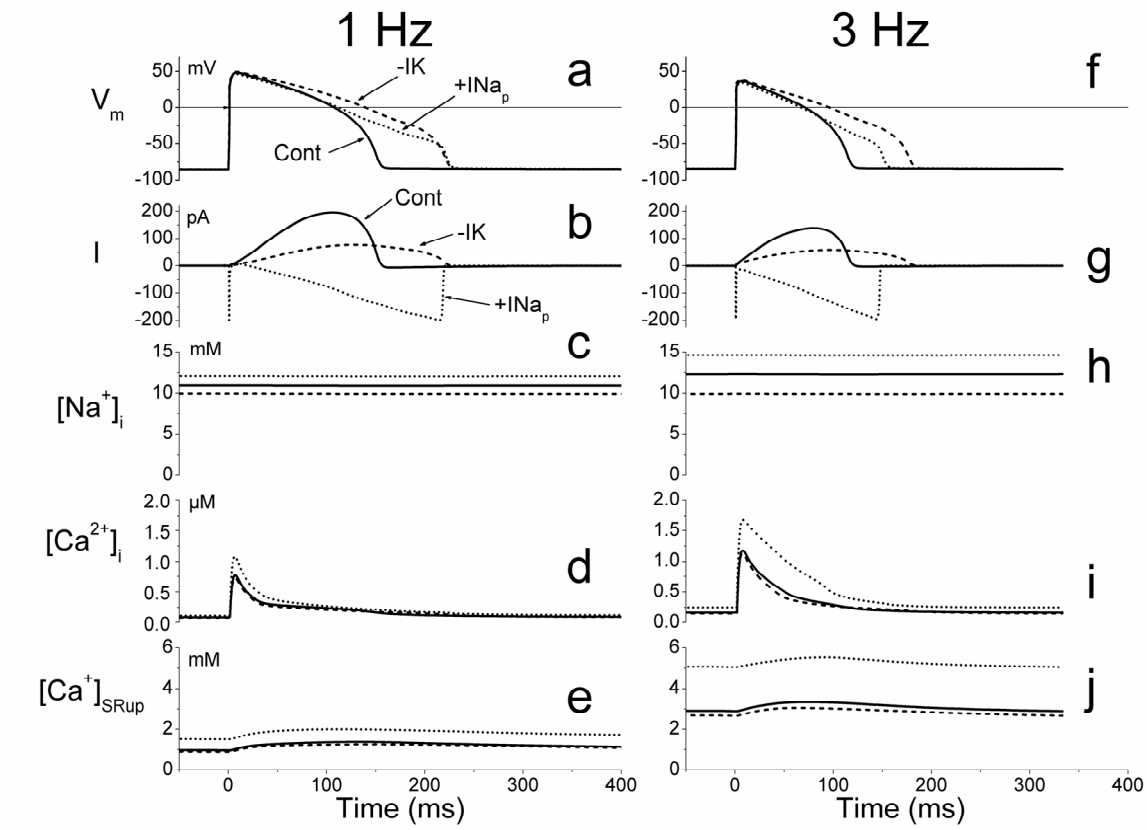

Figure 4 Christé et al. PBMB 2007

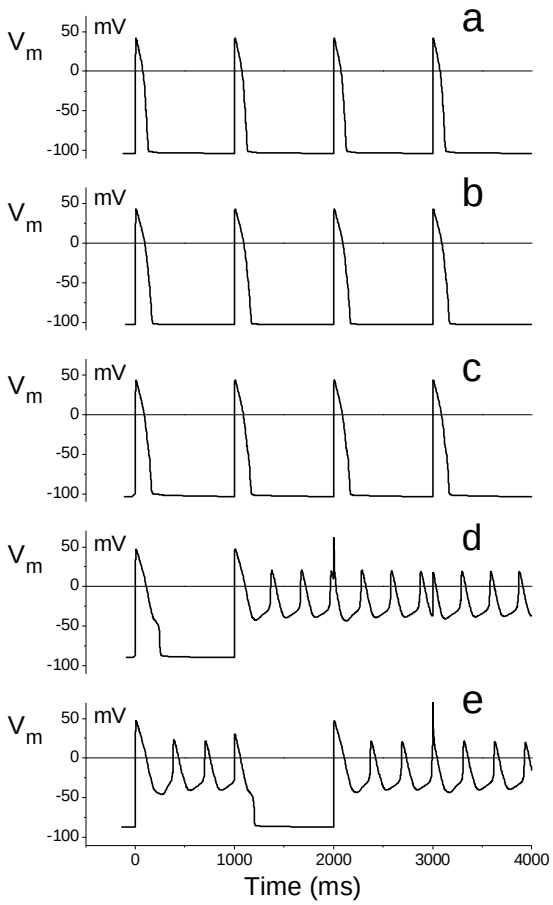

Figure 5 Christé et al. PBMB 2007